PHYSICAL REVIEW A VOLUME 3, NUMBER 6 JUNE 1971

Sound Propagation in X-Ray-Oriented Single Crystals of hcp Helium-4 and bcc Helium-3†

D. S. Greywall*
Physics Department, Indiana University, Bloomington, Indiana 47401
(Received 17 November 1970)

Measurements of the longitudinal and transverse sound velocities in x-ray-oriented single crystals of hcp ^{4}He (19.0–20.5 cm^3/mole) and bcc ^{3}He (21.6 cm^3/mole) are reported. These data are used to compute the respective second-order adiabatic elastic moduli. The moduli for ^{3}He imply an extremely soft transverse mode in the ⟨101⟩ directions and thus demonstrate that the low-temperature bcc-^{3}He specific-heat anomaly is due to an anomalous phonon spectrum. The Debye temperatures and volume compressibilities determined by the elastic moduli for both bcc ^{3}He and hcp ^{4}He are in agreement with values determined by other methods.

I. INTRODUCTION

In the early experiments on solid helium, no special care was taken to ensure single-crystal growth, the blocked-capillary method with growth at constant volume being employed most often.[1] Nevertheless it was found that there was a strong tendency for the solid to crystallize into a few large crystals rather than into a polycrystalline sample. This tendency for large crystals to form is indeed fortunate; for, even though it has made attempts to form powder samples for the most part unsuccessful, it makes possible—with reasonable effort—the growth of large *single* crystals which are desired for most experiments.

The controlled growth of helium crystals was first reported by Shal'nikov.[2] Growing the crystals in a glass tube, he was able to monitor the growth of the samples visually, but found that it was difficult to prevent unwanted nucleation on the walls of the tube when growing the crystals by increasing the pressure. Mezhov-Deglin[3] in his attempts to measure the thermal conductivity of hcp ^{4}He, expanded upon Shal'nikov's techniques and developed a method of growing crystals at constant pressure. Using this method he was able to produce crystals of very high quality, but as determined only by the conductivity measurements themselves. These two works have proved to be the pioneering efforts in the growth of high-quality helium crystals. The work presented in this paper as well as most other recent work on single helium crystals relies heavily on this foundation, although some success has been reported on samples grown from the superfluid at constant temperature.[4,5]

X-rays have been used to determine the structure of all solid phases of both ^{3}He and ^{4}He,[6] but outside of the recent work on the thermal conductivity of hcp ^{4}He by Fain and Lazarus,[7] x-ray methods have not been used to orient single-crystal helium samples on which other measurements of anisotropic properties were made. The number of experiments performed on oriented single crystals of helium is rather small with all of the work until now being confined to hcp ^{4}He where, with the exception just mentioned, either neutron diffraction[8,9] or optical birefringence[5,10] has been the orienting mechanism. The use of these methods is, however, very limited. Neutron scattering cannot be used on solid ^{3}He because of its very large neutron cross section; optical birefringence is not present in the cubic phases. It has been suggested that the large anisotropy in the thermal conductivity in hcp ^{4}He be used as a means of orienting samples for other measurements,[11,12] but it appears that if these crystals were not long narrow single crystals of the highest quality, there would be a large amount of ambiguity in the orientation. The thermal conductivity in the cubic system is isotropic. Thus, although there are inherent problems of x-ray scattering from helium with its low scattering power and large zero-point motion, probably this method, at least at the lower pressures, is the most direct and generally useful approach to determining crystal quality and orientation.

The first measurements of the velocity of sound in solid helium were reported in 1961 by Vignos and Fairbank.[13] Using the time-of-flight pulse technique at a carrier frequency of 10 MHz and working at pressures up to 150 atm they were able to obtain longitudinal velocity measurements in solid ^{4}He, ^{3}He (98%), and ^{3}He-^{4}He mixtures.[14] However, their measurements were performed using a cell immersed directly in the helium bath, and although special precautions were taken to keep the fill line open during the freezing process, there was no control over the crystal growth and nothing at all could positively be said about the quality or orientation of the samples. The authors, nevertheless, concluded from their observations that

their samples were probably either one or several large single crystals which grew with a preferred orientation relative to the freezing chamber and that the experimental scatter of up to 12% was due to anisotropy in the velocity of sound.

Quite similar measurements were made by Lipschultz and Lee[15,16] on both solid ^{3}He and ^{4}He. In addition, however, satisfactory *transverse* measurements were also performed on bcc and hcp ^{4}He grown from the superfluid. Again there was no way to absolutely determine the quality or orientation of the solid helium samples, although the velocity data indicated that possibly the samples were preferentially oriented single crystals.

Relying on the foundation that has developed in the growth and orientation of single helium crystals, the more recent work in this area has been carried out on oriented single crystals of hcp ^{4}He where the meaningful interpretation and comparison with theory are possible. These experiments include the investigations of the phonon spectrum using inelastic neutron scattering[8,9] and the sound-velocity measurements on birefringence-oriented crystals by Wanner and Franck[10] and by Crepeau *et al.*[5]

In the present work longitudinal and transverse velocity measurements are reported for both low-density, hcp-^{4}He, and bcc-^{3}He crystals whose quality and orientation were determined using x rays.

Preliminary reports of portions of this work have previously been published.[17,18]

II. APPARATUS

The solid helium samples were grown in a small acrylic plastic cell which sat near the bottom of the evacuated center bore of a Mössbauer-type Dewar with horizontal optical access. The cell was thermally connected to a helium pot located inside the center bore. The pressure needed for the solidification of helium was provided by means of a helium "gasifier"[19] located in a second Dewar and was propagated through a capillary line connecting the "gasifier" to the cell. The x-ray tube was mounted above the Dewar—the beam traveling almost the length of the cryostat (approximately 30 in.) before striking the crystal. A Polaroid x-ray camera was mounted under the Dewar to intercept the scattered radiation passing through the beryllium windows in the bottom of the Dewar. A 20× microscope could be used to visually monitor the growth of the crystals.

The apparatus used is represented in Fig. 1. M_C and M_G are 0–1500-psi Heise pressure gauges which monitored the pressures in the cell and "gasifier," respectively. The high-pressure line connecting the "gasifier" to the cell was 0.040-in.-i.d., 0.072-in.-o.d. stainless-steel capillary tubing. The valves in this line were stainless-steel bellow valves. To help maintain the pressure constant during crystal growth, the 25-cm^3-volume reservoir was added to the system. The vapor pressure over the liquid helium in the "gasifier" Dewar and in the pot was controlled by a Walker regulator[20] and was measured using a Wallace and Tiernan FA160 0–50-Torr vacuum gauge.

Cryostat

The detailed drawing of the cryostat (Fig. 2) is, for clarity, shown rotated 90° with respect to the axis of the optical windows in the tail section of the Dewar. The helium pot was constructed of brass and had a volume of approximately 0.6 liter. This large volume allowed running times of more than 12 h even with the numerous periods of heat input necessary for the melting of each crystal. To admit the x rays to the cell, a $\frac{1}{2}$-in.-diam tube was passed through the center of the pot. On the bottom end of this tube, a $\frac{1}{16}$-in. collimator was mounted. The whole insert was centered in the Dewar bore with two heavy copper baffles to which silver-plated beryllium-copper fingers were soldered to provide a snug fit with good thermal contact to the bore tube. The two copper baffles thermally anchored to the liquid-helium and liquid-nitrogen reservoirs, respectively, also served to heat sink the fill line and electrical leads running to the cell. To prevent any heat from flowing directly to the cell through the rf lead, the lead was passed through the pot. The center conductor was ther-

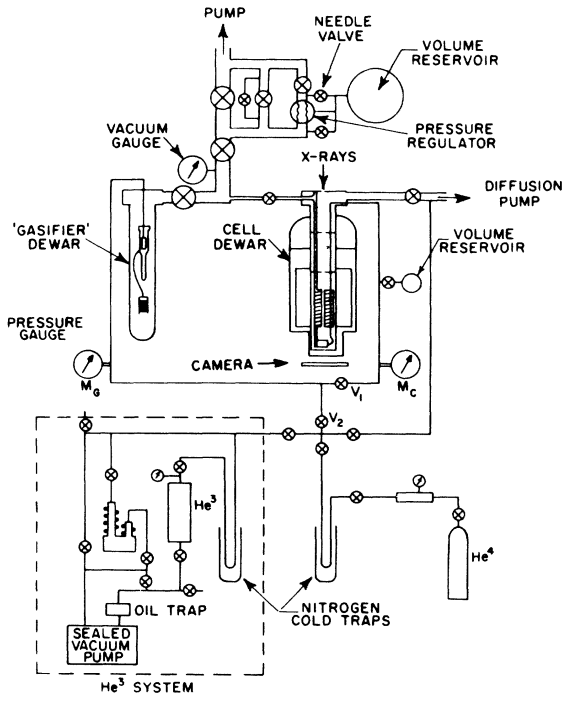

FIG. 1. General experimental setup.

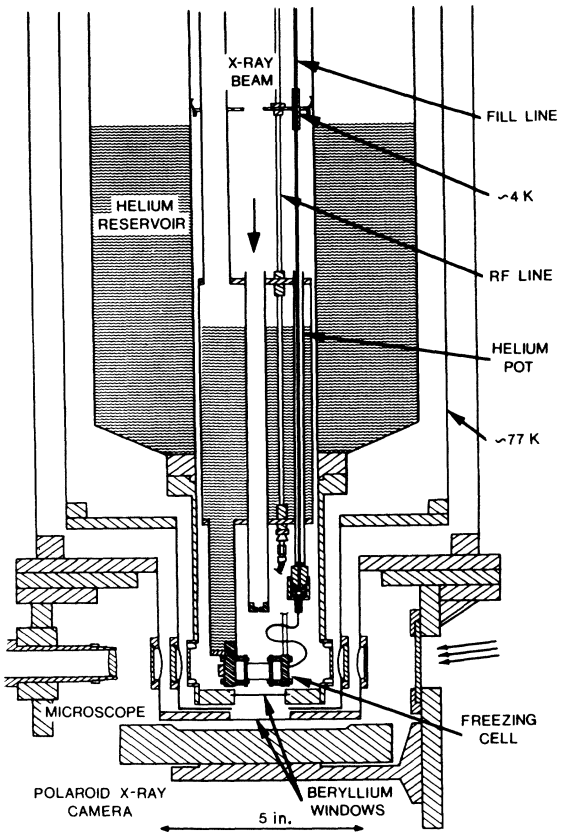

FIG. 2. Cryostat.

mally anchored to the $\frac{1}{8}$-in. stainless-steel tubing outer conductor, in contact with the helium in the pot, by high-thermal-conductivity Epoxy (Stycast 2850 FT[21]).

Freezing Cell

A drawing of the helium freezing cell is shown in Fig. 3. The cavity had a diameter of approximately $\frac{5}{8}$ cm and a volume of approximately $\frac{5}{8}$ cm^3. The body of the cell was turned from Polypenco cast-acrylic plastic.[22] The two major reasons for selecting this material were its low x-ray absorption coefficient and its low thermal conductivity. The latter property was important in that it forced the heat of fusion to be carried away through the growing crystal, helping to ensure single-crystal growth. Other qualities contributing to the choice of this material were its hardness, which permitted fine polishing; its strength, which allowed keeping the wall thickness to 0.040 in. and its transparency, which permitted visual inspection of crystal growth.

The end cap on the freezing end of the cell was made of copper, the opposite cap of brass. After the caps were turned and the screw holes bored, the excess material was cut away leaving the outside of the plug square in shape. On the top of the copper plug, however, a $\frac{1}{4}$-in. rod $\frac{1}{2}$ in. long was left remaining. This rod was then fit into a hole in the cold finger and silver soldered in place; the liquid helium in the pot made direct thermal contact to the end cap. Removing the material from the bottoms of the caps allowed placing the cell very near the beryllium windows in the bottom of the Dewar. To help in the nucleation of a single seed, part of the freezing face of the copper end cap was cut away and replaced with a stainless-steel washer $\frac{1}{16}$ in. thick, leaving the face flat as before but now with only a $\frac{1}{8}$-in.-diam copper surface making direct contact to the helium in the cell. As the temperature of the end cap was lowered, the temperature of the washer lagged behind forcing the nucleation of the crystal to take place on the small copper freezing face.

Sealing between the end caps and the cell body was achieved using O rings formed from 0.025-in. indium wire. The sealing surfaces of the cell body were prepared by polishing against a glass plate frosted using No. 600 carborundum grit. During assembly a light coating of Apiezon-N grease was applied to these surfaces.[23] With an O ring in place, four No. 6-32 nylon screws and a U-shaped brass collar placed behind one of the shoulders of the body were then used to draw the body evenly against the end plug. Starting with 8 lb in., the torque on the nylon screws was increased in steps of 2 lb in. up to 20 lb in. With a vacuum pulled on the cell it was left untouched for approximately 12 h, giving time for both the indium and grease to flow. The screws were then again torqued to 20 lb in. before placing the cell in the Dewar. The seals were 100% reliable.

The X-cut (compressional) and AC-cut (shear) 10-MHz quartz transducers used were $\frac{3}{8}$ in. in diameter, gold plated over the entire inner surface

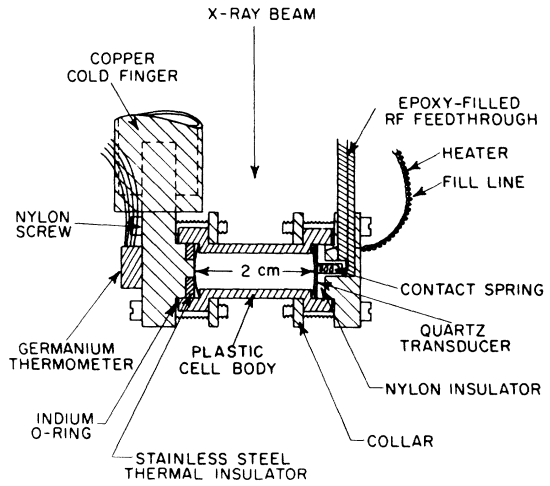

FIG. 3. Details of the freezing cell.

and on a $\frac{1}{4}$-in.-diam pad concentric with the transducer on the outer surface. Electrical contact was made to this pad via a small beryllium-copper spring (0.080-in. o.d.) which was electrically separated from the end cap at ground by a nylon insulator. The No. 33 bare copper-wire lead soldered to this spring was passed out of the cell through a thin-walled $\frac{1}{8}$-in.-diam stainless-steel tube 2 in. long soldered into the brass end cap. Prior to filling the tubing with Stycast 2850 FT Epoxy, the inside and outside of the tubing were sanded with fine emery cloth and washed thoroughly with acetone. Using a long-needled syringe, the Epoxy was injected filling the tubing to overflowing so that the Epoxy also coated at least the top $\frac{1}{2}$ in. of the outside of the tubing. The Epoxy was allowed to cure at room temperature for at least 48 h. The transducer was held against the nylon insulator with a small flat clamping spring ($\frac{1}{4}$-in. i.d., $\frac{3}{8}$-in. o.d.) spark cut from 0.005-in. beryllium-copper. Electrical connection between the helium side of the transducer and the end cap was made through this spring, silver conductive paint brushed onto the inner surface of this end of the cell and the indium O ring. To connect the volume caught behind the transducer to the main volume, shallow grooves were milled on the face of the nylon piece.

The cell was joined to the stainless-steel capillary fill line at the coupling extending below the pot shown in Fig. 2 with a 13-cm length of 0.018-in.-i.d., 0.028-in.-o.d. copper-nickel capillary tubing. The capillary was soldered into the brass cap as shown in Fig. 3. The gas entered the main cavity by flowing around the nylon insulator and transducer. A 500-Ω Evanohm heater wound around the capillary was used to free the line of solid helium when the melting of the solid was desired. The fill line above the coupling was thermally anchored to 4 and 77 K through the heavy copper baffles which were anchored to the liquid-helium and liquid-nitrogen reservoirs, respectively. The only thermal connection to the helium pot was at the coupling which was hung on the end of a 3-cm length of 0.300-in.-i.d., 0.306-in.-o.d. Cu-Ni tubing.

"Gasifier"

The "gasifier" used to generate the necessary pressure was a copy of the device designed and built by Tkachenko and Filimonov[19] (see Fig. 4). It consisted of a glass tube in which was suspended a pressure bulb connected via the capillary line to the cell and a helium pump joined to the glass tube by a short length of capillary which was used to fill and empty the glass tube.

The whole assembly was placed in a Dewar filled with helium II to a level not higher than the bottom of the pressure bulb. When a current was passed through the pump heater which was separated from the main bath of helium by a super leak, the thermomechanical effect caused the liquid to be forced into the glass tube. Pure helium gas could then be condensed into the pressure bulb. When the pressure was desired, the pump heater was turned off, the helium allowed to drain from the glass tube and heat applied to the pressure bulb, causing the liquid to "gasify." The purpose of the spiral fin and the tail was to help stabilize the pressure by compensating for the heat input down the pressure-transmitting capillary.

The stainless-steel bulb used in the present setup was 5 in. long with a volume capacity of 6 cm^3 and a spiral fin 0.200 in. high and 0.020 in. thick. Parallel to the fin a 200-Ω Evenohm heater was wound. The tail was a $5\frac{1}{2}$-in. piece of 0.080-in. piano wire soldered into the bottom of the bulb. The stainless-steel pump was 2 in. long and 0.800 in. in diameter, the super leak being a plug of No. 480 carborundum grit held in place by sandwiches of fine monel screen and cotton. The pump heater was a 2.3-K wire-wound resistor.

The "gasifier" proved to be a very inexpensive, reliable, and clean device which was very simple to build and easy to use and control.

Electronics

A single-ended pulse-echo method was used to measure the velocity of sound in the helium crystals. The circuitry is shown in Fig. 5. A 10-MHz pulse of 1-μsec duration was delivered to the cell transducer from the pulsed oscillator every millisecond. The signals, the direct pulse (clipped) plus the echos, were mixed with the 20-MHz cw signal of the local oscillator and then after pre-

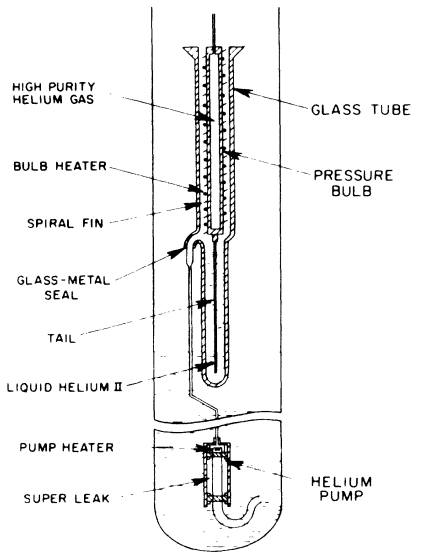

FIG. 4. Helium "gasifier."

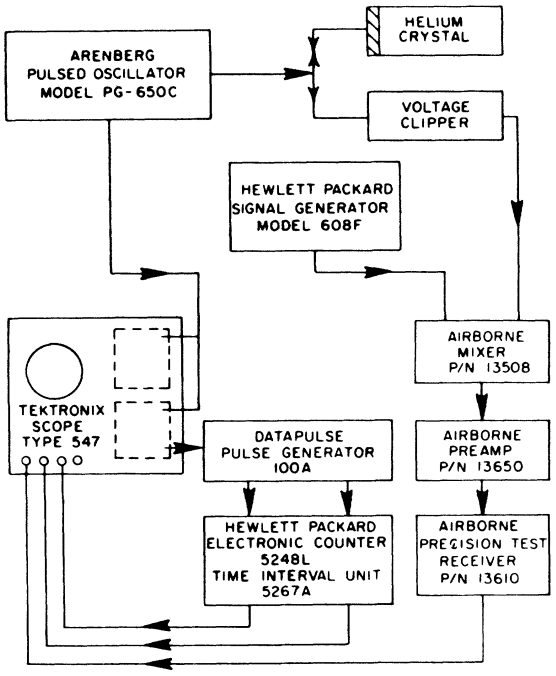

FIG. 5. Block diagram of the electronic circuitry.

amplification fed into a narrow-band receiver tuned to 30 MHz. The output signal was monitored on the four-trace oscilloscope triggered by an advanced signal from the transmitter. An adjustable delayed trigger from the oscilloscope activated a pulse generator which was capable of putting out two pulses: one nearly simultaneous with the delayed trigger of the oscilloscope, the other a variably delayed pulsed. These pulses triggered the opening and closing of the timing gate of the counter. Both the opening and closing of the gate were marked with sharp output spikes which were monitored on the oscilloscope. Thus, by varying the delayed trigger of the scope, the "open" spike could be lined up with the leading edge of one received pulse; the variable delay on the pulse generator could then be adjusted to line up the "stop" spike with another echo, the counter reading the time interval between the two events to within a few hundredths of a microsecond.

III. EXPERIMENTAL PROCEDURE

In preparation for an experimental run, the capillary line joining the cell and "gasifier" and the pure ^{4}He cylinder or ^{3}He system was pumped for at least 48 h with the vacuum gauge at the diffusion pump reading 10^{-6} Torr (refer to Fig. 1). The "gasifier" and cell Dewars were then cooled to liquid-nitrogen temperature. After 24 h the capillary system was separated from the pump and liquid helium transferred into both Dewars and the helium pot. As the mechanical pump lowered the temperature of the liquid helium in the "gasifier" Dewar and in the pot, the high-purity helium gas (Linde research-grade ^{4}He or Monsanto low-^{4}He-content ^{3}He) was bled through the nitrogen cold trap into the cell and "gasifier" pressure bulb.

If ^{4}He crystals were to be grown at a constant working pressure with a corresponding freezing temperature T_F, less than the ^{4}He superfluid transition temperature T_λ, the "gasifier" and pot temperature were lowered to approximately $T_F + 0.1$ K $< T_\lambda$ and held at this point with the temperature regulator. The glass tube of the "gasifier" was then filled with helium II with a dissipation of ~ 20 mW of power in the pump heater. When the condensation was complete, the "gasifier" bulb and cell filled with high-purity liquid helium, valve V_2 was closed, separating off the cell-"gasifier" system. After the "gasifier" pump heater was turned off and the glass tube allowed to drain, the "gasifier" bulb heater was turned up gradually until the rate of pressure increase was approximately 2 atm/min. When the working pressure was reached, it was maintained manually by adjusting the bulb-heater current while the pot temperature was lowered almost linearly with a single setting of the needle valve on the Walker regulator. When the crystal was just completed, valve V_1 was closed, completely isolating the cell system from the rest of the apparatus.

For higher-pressure ^{4}He crystals with $T_F > T_\lambda$, the procedure had to be slightly modified due to the nonfunctioning of the "gasifier" pump above T_λ. In this case, as above, the system was pumped to some temperature below T_λ, the pure helium condensed into the "gasifier" and cell, and V_2 closed; but now the vacuum pump was separated from the system and the vapor pressure over the pumped helium allowed to rise. This was hastened by using the fill-line heater and by slowly bleeding helium gas into the pumping lines. When the temperature was approximately 0.1 K above T_F, it was held with the regulator. The heater on the "gasifier" bulb then raised the pressure up to the working pressure which was maintained manually as the pot temperature was lowered. V_1 was closed when the crystal was complete.

The ^{3}He crystals were grown at a working pressure of 950 psi only. This pressure corresponds to a $T_F < T_\lambda$ but with the liquid-gas expansion only $\frac{5}{8}$ that of ^{4}He, the first method described above was only capable of producing pressures of ~ 800 psi even with the volume reservoir closed off from the capillary line. The working pressure of 950 psi had to be achieved in two steps. With the cell at a temperature of ~ 1.2 K and filled with liquid ^{3}He at ~ 800 psi, V_1 was closed. The "gasifier" pump

then refilled the glass tube, condensing the gas in the "gasifier" and in the capillary up to valves V_1 and V_2. V_2 was then opened to allow more gas to condense into the gasifier. When this process was complete, V_2 was closed, the pot temperature raised above T_F and the bulb heater gradually warmed. At a pressure of 800 psi, V_1 was opened. The pressure in the cell was then taken to 950 psi. V_1 was closed when the crystal was complete.

With the ^{4}He or ^{3}He crystal completely filling the cell and the freezing end of the cell approximately $\frac{1}{2}$ K below the melting temperature, the sound-velocity measurements were made and the x-ray photographs taken.

The crystal was then melted by first using the fill-line heater (~ 1 mW) and then isolating the pump from the system allowing the temperature to rise above T_F. The temperature was held by the regulator. The heater was left on for 20–30 min. In another 20–40 min, the temperature was again lowered freezing a second crystal. Since V_1 remained closed throughout the melting and refreezing process, the change in volume on freezing produced a corresponding change in pressure. The volumes of the Bourdon tube of the pressure gauge and the volume reservoir, used only during the growth of ^{4}He crystals, were such that this change in pressure was approximately 4% for all crystals.

IV. RESULTS AND DISCUSSION

Crystal Growth and Orientation

In the course of this work, a total of 237 hcp-^{4}He and 97 bcc-^{3}He crystals were grown. All but eight of these crystals were grown at nearly constant pressure according to the procedure discussed in Sec. III. The ^{3}He crystals were grown under a single working pressure of 950 psi which corresponds to a molar volume of 21.6 cm^3.[24] The ^{4}He samples were grown under pressures of 473 psi (190 crystals), 614 psi (12 crystals), 775 psi (13 crystals), and 950 psi (14 crystals) which correspond to molar volumes of 20.5, 20.0, 19.5, and 19.0 cm^3, respectively.[25] The eight remaining ^{4}He crystals were grown from the superfluid at 1.2 K by increasing the pressure.

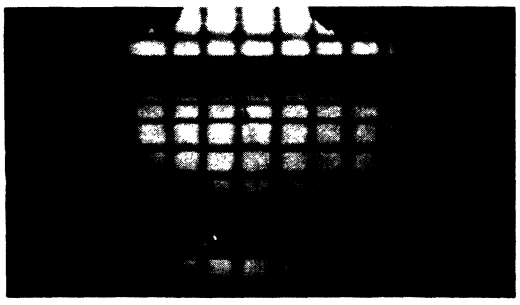

FIG. 6. Photograph taken during the growth (at constant pressure) of a solid helium sample. The solid is to the left of the nearly vertical solid-liquid interface in the middle of the photograph.

The photograph in Fig. 6 was taken during the growth of a helium crystal at constant pressure. The grid of $\frac{1}{16}$-in. squares scribed on a flat light-diffusing screen was positioned just in back of the cell. The heavy dark horizontal lines correspond to the top and bottom edges of the cylindrical plastic cell body (refer to Fig. 3). The liquid-solid interface, tracing out a constant-temperature surface, moved across the cell at a nearly linear rate corresponding to the very nearly linear decrease in the temperature of the cold finger.[26] The interface appeared to be most visible during the growth of the highest-pressure ^{4}He crystals and the least visible during the growth of the ^{3}He samples. All of the crystals grown at constant pressure were optically clear independent of the quality determined by x-ray analysis.

In an attempt to grow extremely poor purposely strained crystals, a few samples of ^{4}He were grown from the superfluid at constant temperature by increasing the pressure rapidly. The solid nucleated on the fill-line side of the cell and rapidly filled the whole cavity as a visually obvious polycrystal. Rapid recrystallization which occurred almost simultaneously with the growth of the solid, however, left the sample perfectly clear within a matter of a few seconds. x-ray photographs showed no Laue spots at all. There was also no electronic signal. In other samples grown from the superfluid in which the pressure was increased at a few psi per minute there was more control over crystal growth with the solid nucleating on the cold-finger side of the cell, but again the x-ray quality of the samples was extremely poor. In all cases crystal clarity provided no information about crystal quality.

Most of the crystals were grown at rates of from (2 cm)/(30 min) to (2 cm)/(60 min) and were of the highest quality as determined by the transmission Laue x-ray photographs. Even with the slight changes in pressure as the helium solidified, most samples appeared unstrained and required no annealing, thus permitting in a few cases as many as 10 or 12 different crystals to be grown in a single day. Because the helium scattering cross section is extremely small, the x-ray beam easily penetrated the $\frac{1}{4}$-in.-diameter crystal sampling *all* of the solid in the path of the beam and producing Laue photographs which provided severe tests of crystal quality. Examples of these photographs are shown in Fig. 7. The slight radial spreading of the diffraction spots is due at least in part to the thickness of the crystals. The photographs were taken at a tube potential of 55 kV and a tube current of 25 mA with an exposure time of approxi-

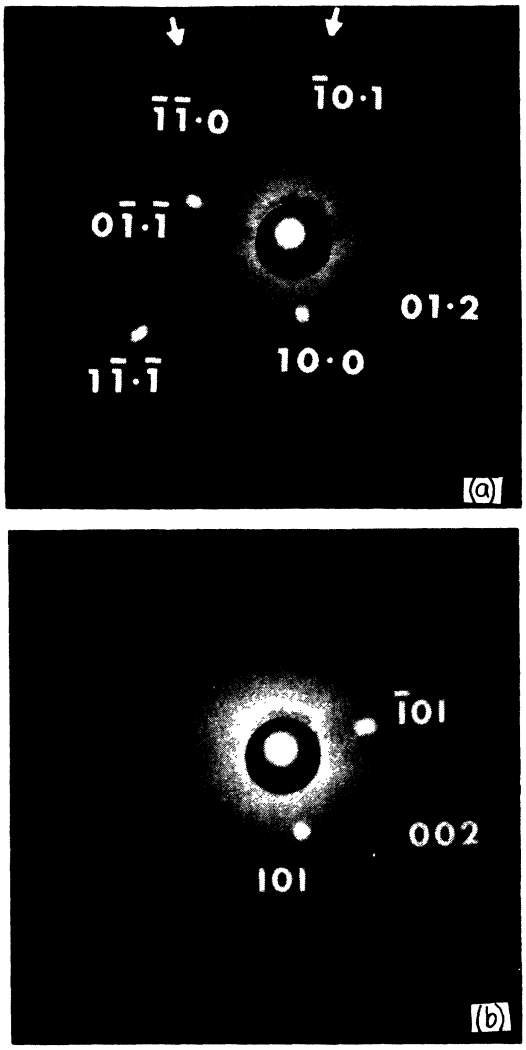

FIG. 7. Transmission Laue photographs of (a) a single hcp-helium-4 crystal (20.5 cm^3/mole) and (b) a single bcc-helium-3 crystal (21.6 cm^3/mole). The crystal-to-film distance was 5 cm.

mately 7 min using Polaroid-type 57 film. The white background scattered from the plastic cell body shows the shadow cast by the beryllium windows. The large bright central spot is an overexposure of the direct beam. The dark annulus about this spot and the four small black dots are due to the construction of the Polaroid camera.

The labeling of the diffraction spots was determined using the usual stereographic projection method.[27] However, a simple calculation of the relative intensities of the spots considering only the structure and temperature factors proved extremely helpful. Neglecting the fact that the beam intensity is a function of the wavelength, the brightest spots in the hexagonal system correspond in order to the $00\cdot2$, $10\cdot1$, $10\cdot0$, and $10\cdot2$ reflections. This information provided a good running start on the determination of the crystal orientations. Most often the brightest spot was a $10\cdot1$ reflection. In the cubic system, the brightest spots are of the 101 and 002 types and differ by a factor of 10 in relative intensity. See Fig. 7(b). An example of the type of stereographic projection made for each crystal is given in Fig. 8.

Of all the crystals grown, sound-velocity data were taken from less than 50%. A large number of the samples were not usable due to poor acoustical bonds to the quartz transducer. Other samples had to be rejected because the Laue photographs did not yield enough information to unambiguously determine the orientation or indicated a polygonal or otherwise polycrystalline structure. The frequency of the occurence of crystal defects seemed to be a function of growth rate. At the slower growing rates, the crystals more often showed severe polygonization (although in all cases this defect was quite rare); at the faster rates, the samples were more often polycrystalline or showed weak electronic signals. The terms "slower" and "faster" refer to optimum growing rates which decreased slightly with pressure and were of the order of (2 cm)/(45 min).

The hcp-^{4}He Laue photographs normally had between three and six spots and usually indicated a crystal whose c axis was nearly parallel to the freezing surface. In fact, 80% of all the usable hcp-^{4}He crystals had their c axis inclined at less than 30° from the freezing surface. Fain and Lazarus[28] have also observed this tendency for the c axis to be perpendicular to the growth direction. Figure 9(a) shows the stereographic projection of the $00\cdot1$ pole of each of the hcp crystals from which data was taken. An attempt was made not to include more than one sample grown from the same seed. The spread of dots parallel to the freezing surface is quite uniform and thus does not indicate any further restriction on the preferred direction of growth. The histogram representing 99 samples, Fig. 9(b), plots in 10° intervals the number of crystals as a function of the angle between the c axis and the cell axis. Only 5% of the samples had a θ less than 30°. Thus, on the few occasions when the c axis did grow nearly parallel to the cell axis, as could be determined immediately from the large longitudinal sound velocity, the crystal was regrown two or three times, each time from a small seed left from the preceding crystal. Here the optical transparency of the cell was extremely important. It was a trivial matter to leave as small a seed as desired. The fact that these seeds yielded crystals of very nearly the same orientation was further indication that the whole solid filling the cell was of the same orientation as that part of the sample x rayed. The highest quality samples

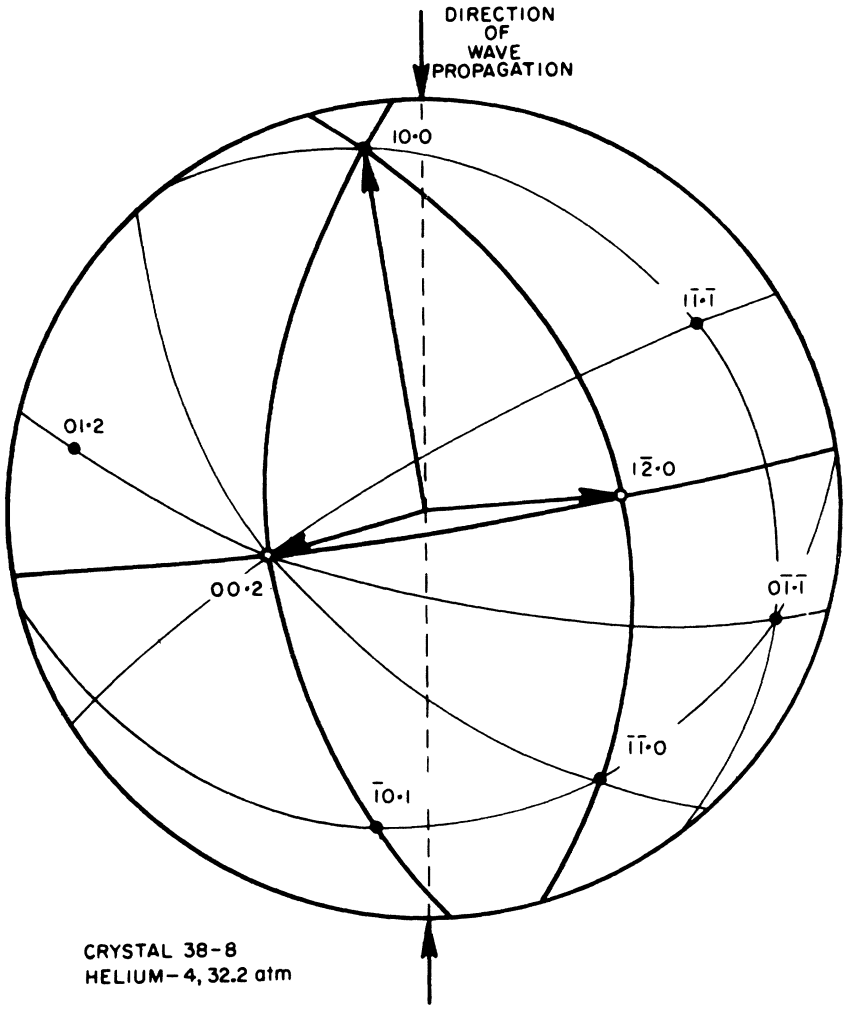

FIG. 8. Stereographic projection corresponding to the hcp-^{4}He Laue photograph shown in Fig. 7(a). The $00 \cdot 2$ and $1\bar{2} \cdot 0$ poles are the results of construction.

grown appeared to be those which grew in the preferred direction. This can also be seen in the sound-velocity data, Fig. 10, which shows more scatter at θ less than 70°.

If crystals grown from the superfluid have the same large probability of not growing with the c axis parallel to the growth direction then one must conclude from the possibilities suggested by Heybey and Lee[4] that the 50% of their samples which showed birefringence phase shifts of less than 5° were polycrystalline. This would be compatible with the difficulty encountered in the present work in the few attempts at growing single crystals from the superfluid.

The bcc-^{3}He Laue photographs most often had only two or three spots which, as in the case of hcp ^{4}He, usually indicated a crystal with a preferred orientation. In all cases the diffraction spots could be classified as either 002 or 101 reflections. The very large difference in the intensities of these reflections made identification of the spots an easy matter; however, in some cases, there was ambiguity in the orientation. If there were only two reflections visible and both were of the 101 type and separated by 60° or 120° there were two orientations of the crystal possible related by a rotation of 60° about the ⟨ 111 ⟩ axis. In such cases data was only taken if the expected sound velocities for the two orientations were sufficiently different so that the actual measurement could be used to definitely rule out one of the possibilities. The preferred orientations of the bcc crystals are shown in the plots of the sound-velocity data, Fig. 11. Each of the dots on the stereographic projections of $\frac{1}{48}$ of the reference sphere gives the direction of sound propagation (or equivalently, the axis of the cell) relative to the principle axis of the crystal. It is clear that the crystals from which velocity data were obtained tended not to grow with the ⟨ 100 ⟩ or the ⟨ 111 ⟩ axis parallel to the cell axis. Two of the three samples which did grow with the ⟨ 100 ⟩ axis parallel to the axis of the cell were grown from the same seed; the third was grown the same day but not consecutively with the first

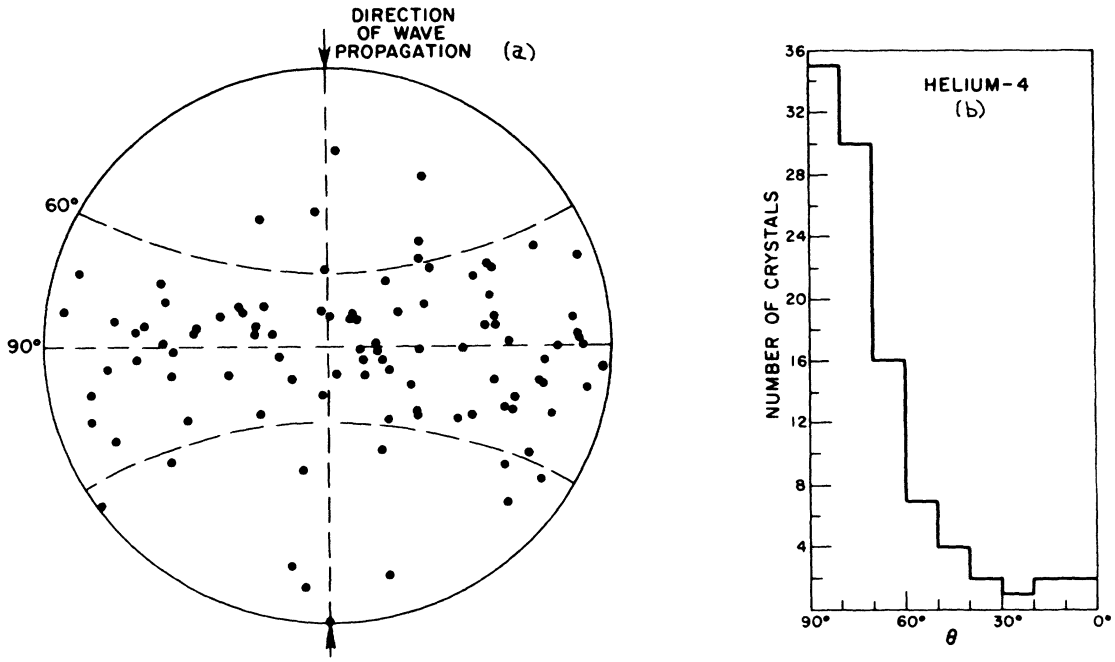

FIG. 9. Plots showing the preferred orientation of hcp-^{4}He crystals. (a) Stereographic projection of the intersection of the c axis of each crystal with the reference sphere (i. e., of the 00•1 poles). (b) Histogram plotting in 10° intervals the number of crystals vs the angle between the c axis and the cell axis.

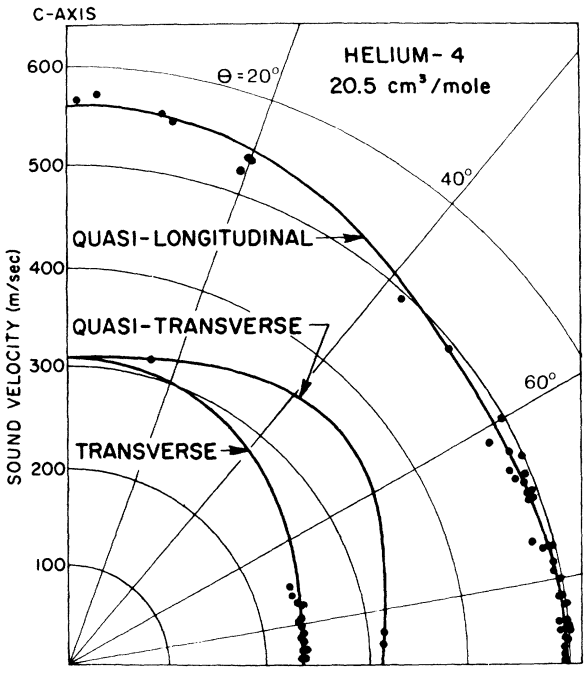

FIG. 10. Polar plot of the longitudinal and transverse sound velocities in hcp ^{4}He at 20.5 cm^3/mole. θ is the angle the propagation vector makes with the c axis.

two. This probably indicates that there was some contamination on the freezing face which caused the crystals to nucleate with this particular orientation. Although it was not the case here, it should be pointed out that it was easily possible to leave a seed unintentionally by not completely melting the preceding sample even when warming the cell from both ends.

Sound-Velocity Measurements and Elastic Constants

Examples of some of the better sound signals received are shown in the oscilloscope-trace photographs in Fig. 12. Although the 10-MHz pulse delievered from the pulsed oscillator was usually only 1 μsec in duration, the actual transmitted pulse was very much longer due to the ringing of the quartz transducer. This, however, in no way affected the velocity measurements; the ringing never disturbed the leading edge of the following echo.

By mounting the cell horizontally with the fill line entering the cavity from behind the transducer, it was hoped that the helium crystal would grow onto the transducer slowly and evenly without trapping any volume of liquid against the transducer and would thus ensure a good crystal-transducer bond enabling transverse as well as longitudinal waves to be propagated. In most cases, provided the samples were grown "slowly enough," longitudinal

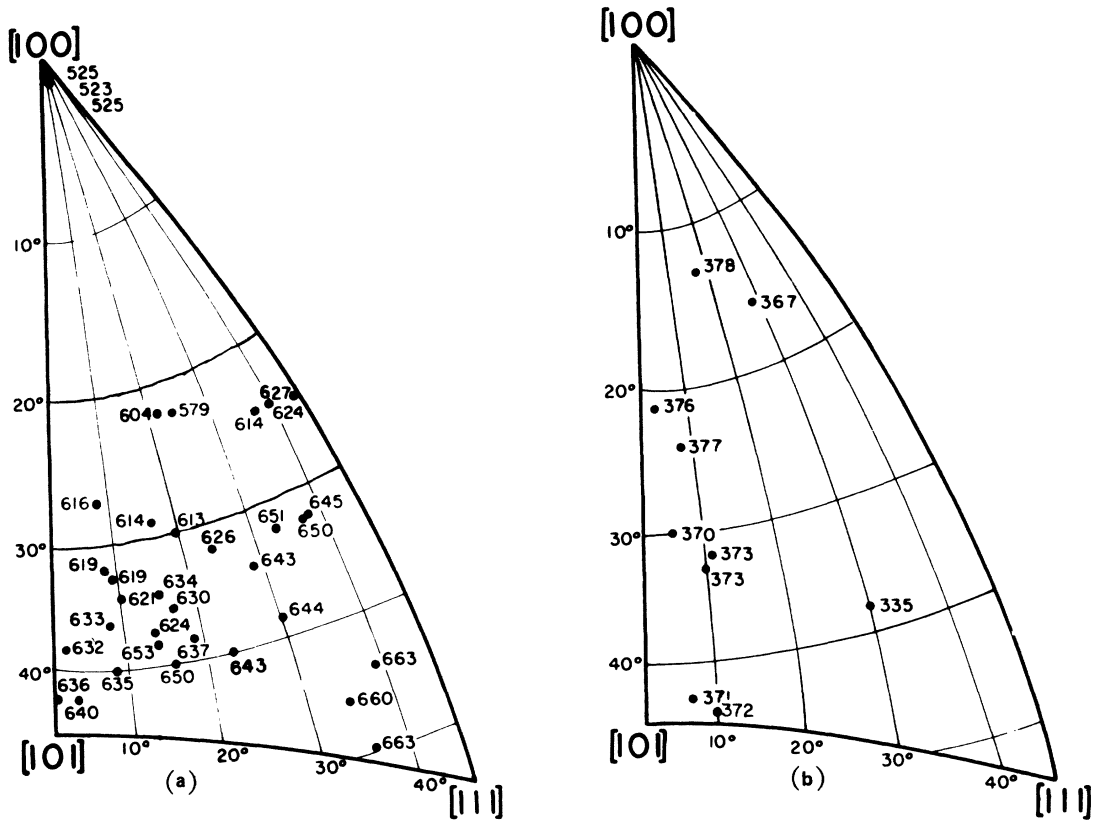

FIG. 11. (a) Longitudinal and (b) transverse (T_1) sound velocities in bcc ^{3}He (21.6 cm^3/mole) plotted in m/sec on stereographic projections of $\frac{1}{48}$ of the reference sphere. Each dot corresponds to a different crystal.

signals were easily generated; on the contrary, however, transverse waves were always very difficult to propagate, although perhaps less so in ^{4}He at the higher working pressures. Many excellent crystals could not be used because no received signals at all were observed. Attempts to obtain signals from these samples by continually increasing the transmitter power resulted in local melting of the helium crystals. This was marked by the onset of uncontrolled transducer ringing. The signals observed with the X-cut transducer were usually purely longitudinal, however with the AC-cut transducer longitudinal as well as transverse signals were obtained, often simultaneously as shown in Fig. 12(c). When both signals were present, "aging" of the crystal frequently strengthened the longitudinal and weakened the transverse signals. In some cases, decaying transverse signals completely disappeared.

Since different pairs of successive echos were separated by slightly different times which showed no apparent pattern, the sound velocities were calculated using the times between the transmitted and the first received pulses. The scatter in the velocity measurements made in this way on different samples was much greater than the error expected from the uncertainty in the time measurement and in the crystal orientation ($\pm 2°$). This scatter may have been due to density gradients remaining in the crystal or possibly to changes in the crystal orientation very near the transducer caused by the change in the shape of the cell.[28] In computing the statistical error in the measured sound velocities normal distributions of the measurements were assumed. The systematic errors introduced by the uncertainty in the length of the sound path is estimated to be less than $\frac{1}{2}\%$.

The sound-velocity data for hcp ^{4}He at a molar volume of 20.5 cm^3 are shown in Fig. 10. Each dot corresponds to a different crystal. Since the velocities of sound in the hexagonal system do not depend on the azimulthal angle, the data are plotted only as a function of θ, the angle the propagation vector makes with the c axis. The "quasi" prefix on two of the curves refers to the fact that even though the displacement vectors must be mutually perpendicular provided no two of the velocities are equal, the displacement vectors need not be parallel or perpendicular to the propagation vector. The pure transverse mode has its displacement

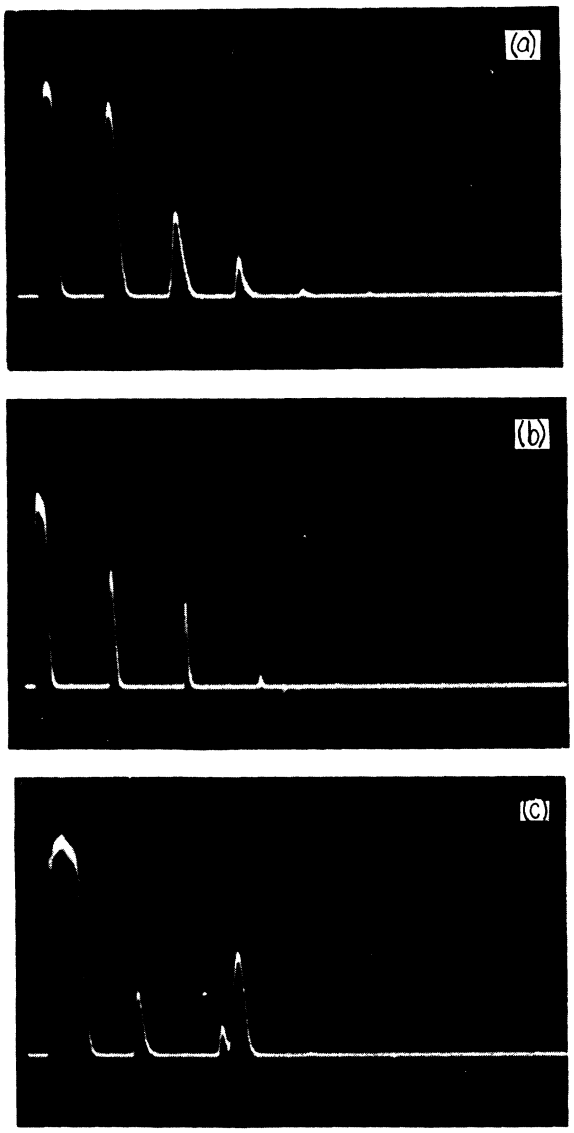

FIG. 12. Oscilloscope traces showing transmitted (first) and received pulses. (a) Longitudinal signal in bcc ^{3}He (50 μsec/division). (b) Transverse signal in hcp ^{4}He (100 μ sec/division). (c) Signal in hcp ^{4}He showing both longitudinal and transverse (last pulse) echoes (50 μsec/division).

vector perpendicular to the c axis. The solid curves in the figure were computed from the five least-squares adiabatic elastic moduli, in units of 10^9 cm^2/sec^2:

$$C_{11}/\rho = 2.39\ (\pm\tfrac{1}{2}\%)\,, \quad C_{44}/\rho = 0.941\ (\pm\tfrac{1}{2}\%)\,,$$

$$C_{66}/\rho = 0.525\ (\pm\tfrac{1}{2}\%)\,, \quad C_{33}/\rho = 3.1\ (\pm 6\%)\,,$$

$$C_{13}/\rho = 0.12\ (\pm 300\%)\,;$$

ρ is the density. The stated errors in C_{11}/ρ, C_{44}/ρ, and C_{66}/ρ were determined using the standard error in the measured sound velocities of 0.6 m/sec. However, as already pointed out, outside of the interval $70^\circ \lesssim \theta \lesssim 90^\circ$, the limited data showed a larger scatter. Thus, it was unreasonable to fix any real meaning to the standard error for $\theta \lesssim 70^\circ$. The errors placed on C_{33}/ρ and C_{13}/ρ were estimated from the scatter in the longitudinal data near the c axis and near 50° to the c axis. Although these two constants could not individually be determined accurately, it was possible to accurately determine their sum through the relation

$$C_{13} + C_{33} = 2(C_{11} - C_{66}) \tag{1}$$

derived by Franck and Wanner[29] from the fact that c/a is a constant independent of molar volume.[30] It is unfortunate that more data could not have been taken near $\theta = 50^\circ$. Had the longitudinal sound velocity here been significantly different from the velocity in the basal plane, it would have been possible to immediately determine that a special (i.e., nonpreferred) crystal had been grown and then to have grown two or three samples from the

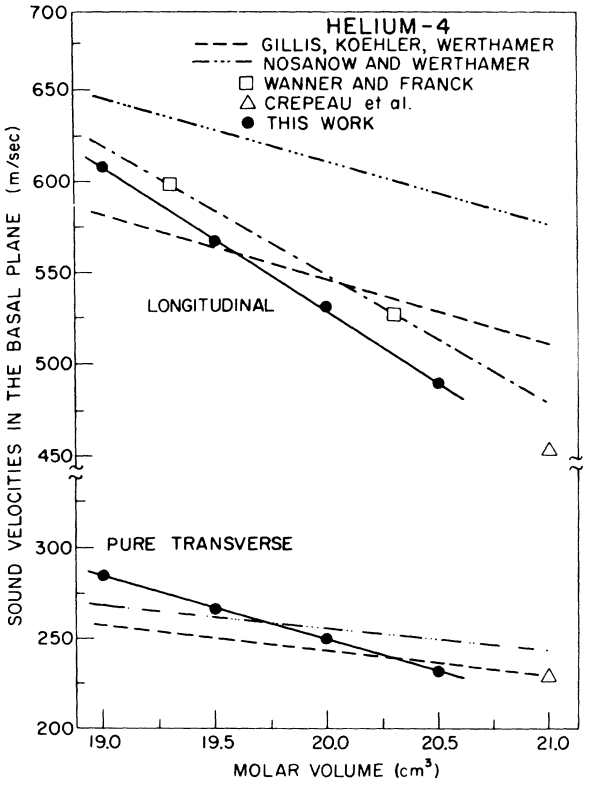

FIG. 13. Density dependence of the hcp-^{4}He longitudinal and pure transverse sound velocities in the basal plane. The theoretical results of Gillis *et al.* (Ref. 31) and Nosanow and Werthamer (Ref. 32) and the experimental results of Wanner and Franck (Ref. 10) and Crepeau *et al.* (Ref. 5) are also indicated.

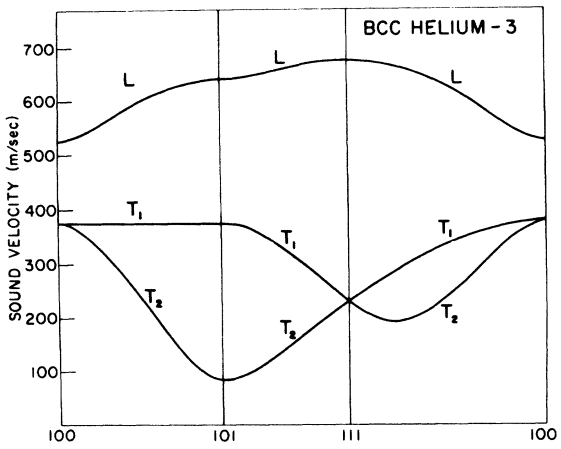

FIG. 14. Longitudinal and transverse sound velocities in bcc ^{3}He (21.6 cm^3/mole) along the edges of the unit triangle shown in Fig. 13. The curves were calculated from the elastic constants determined by the velocity measurements.

same seed. This was possible with the crystals oriented such that the sound propagation was along the c axis; however, very little could be said about the orientation of the former crystals until the Laue photographs were actually analyzed.

The density dependence of the quasilongitudinal and the pure transverse sound velocities in the basal plane is shown in Fig. 13. The theoretical results of Gillis, Koehler, and Werthamer[31] (collective picture) and of Nosanow and Werthamer[32] (single-particle picture) and the experimental results of Wanner and Franck[10] and of Crepeau *et al.*[5] are also indicated. The predicted density dependence is too weak. Gillis *et al.* have pointed out that this is probably associated with several aspects of the treatment of short-range correlations, although it may be that the anharmonic corrections are also important. The measurements of Crepeau *et al.* on helium crystals grown from the superfluid are in fair agreement with the present work; however, the longitudinal velocities given by Wanner and Franck are noticeably higher. This discrepancy is probably in part due to the fact that their values in the basal plane had to be extrapolated.

The sound-velocity data for bcc ^{3}He at a molar volume of 21.6 cm^3 are plotted on stereographic projections of $\frac{1}{48}$ of the reference sphere in Fig. 11. Each dot corresponds to a different crystal and represents the direction of sound propagation. The number associated with each dot gives the velocity in meters per second. As was pointed out in Sec. III, the crystals which yielded velocity data tended to grow such as to avoid having the $\langle 100 \rangle$ or $\langle 111 \rangle$ axis along the axis of the cell. This may explain, at least partially, why the previous work on unoriented ^{3}He crystals[14] did not indicate a large anisotropy in the longitudinal velocity of sound. The range of velocities in the preferred region is only ~30 m/sec as compared with an actual anisotropy of ~125 m/sec.

The longitudinal and transverse sound velocities along the edges of the portion of the reference sphere shown in Fig. 11 are plotted in Fig. 14. The curves were calculated using the three adiabatic elastic moduli determined by a least-squares fitting of the data.[33] In units of 10^9 cm^2/sec^2,

$$C_{11}/\rho = 2.71 \pm 0.01 ,$$

$$C_{12}/\rho = 2.59 \pm 0.06 ,$$

$$C_{44}/\rho = 1.42 \pm 0.01 .$$

The errors correspond to a standard error in the velocity measurements of 1.15 m/sec. This figure shows more clearly the large anisotropy measured in both the longitudinal (L) and higher-frequency transverse (T_1) mode. It also shows the very large anisotropy in the T_2 transverse mode necessarily implied by the data. The very low velocities (~80 m/sec) near the $\langle 101 \rangle$ direction are very interesting in that besides being important in the determination of thermodynamic properties, they also give insight into the nature of the second-nearest-neighbor interaction which accounts for

TABLE I. Theoretical sound velocities in m/sec along symmetry directions in bcc ^{3}He.

	Experiment	Horner (Refs. 37 and 38)	Koehler (Ref. 36)	DeWette *et al.* (Ref. 35)
Direction	21.6 cm^3/mole	21.6 cm^3/mole	22.5 cm^3/mole	21.6 cm^3/mole
Longitudinal				
⟨100⟩	520	~420	559	~600
⟨101⟩	638	520	642	715
⟨111⟩	672	550	668	750
Transverse				
⟨100⟩	377	340	393	435
⟨101⟩	78, 377	120, 340	232, 393	200, 435
⟨111⟩	226	220	296	300

the stability of the bcc lattice.

It should again be noted that the velocity of the ⟨101⟩ soft shear wave has been calculated using velocities of waves propagating in other modes and in other directions. No direct measurements of the very slow sound velocities were made. An inability to propagate very soft ⟨101⟩ shear waves has also been reported by Testardi *et al.*[34] in their work on V_3Si at low temperatures. Thus, it appears that the present failure to propagate this mode may not be attributed to a peculiarity of solid helium alone.

The theories of solid ^{3}He at large molar volumes which do not treat the anharmonic corrections[35,36] predict phonon spectra with transverse sound velocities very much different from those measured. The most serious discrepancy is in the ⟨101⟩ direction. Recently, however, Horner[37,38] and Koehler and Werthamer[39] have made preliminary calculations of the leading anharmonic correction to the phonon spectra. They find that this correction shifts the frequency of the soft ⟨101⟩ transverse mode by a factor of approximately 2, bringing the theory into better agreement with experiment. See Table I.

Debye Temperature

The value of the Debye temperature at absolute zero can be determined using the elastic constants since at very low temperature only the lattice waves of nearly infinite wavelength contribute to the specific heat. At $T = 0$,

$$\Theta_D = (\hbar/k_B)\,(18\pi^2 N)^{1/3} I^{-1/3}\,, \tag{2}$$

where

$$I = (1/4\pi)\int \sum_i (1/v_i^3)\, d\Omega\,,$$

k_B is Boltzmann's constant, v_i are the longitudinal and transverse (2) sound velocities, and N is the number of atoms per unit volume.

Numerical integration of I using a half-degree interval for the single angle variable in the hexagonal system yields a Θ_D of 28.8 K for solid ^{4}He at 20.5 cm^3/mole. The three sound velocities were determined as a function of the propagation direction using the relations in terms of the elastic constants given by Fedorov.[40] The sensitivity of Θ_D to errors in the elastic moduli was checked by independently changing the values of C_{66} and C_{13}. Since C_{66} determines the slowest velocities, Θ_D depends most strongly on this modulus. However, the largest uncertainties are in C_{13}. Changing these moduli by amounts equal to the stated errors resulted respectively in 0.1 and 1% changes in Θ_D. Taking into account the possible systematic error, it is thus estimated that Θ_D is accurate to better than 2%.

The values of $\Theta_D(V_M)$ at the higher densities considered can be simply computed in terms of Θ_D (20.5 cm^3): The longitudinal and pure transverse velocities in the basal plane over the range of molar volumes considered are very nearly linearly dependent on the molar volume with the two velocities at 19.0 cm^3/mole each being 1.23 times greater than the corresponding velocities at 20.5 cm^3/mole. Limited data also indicates that the longitudinal and transverse velocities along the c axis differ over the same extremes of molar volume by nearly the same factor. Since Θ_D is not sensitive to changes in C_{13} it is reasonable when calculating Θ_D to assume that the longitudinal velocity in the ⟨10·1⟩ direction, for example, obeys the same type of density dependence. This is equivalent to assuming that all of the velocities obey the relation

$$v(\theta, V_M) = a(V_M)\, v(\theta, 20.5)$$

or that the elastic moduli obey the relation

$$C_{\alpha\beta}(V_M) = (20.5/V_M)\, a^2(V_M)\, C_{\alpha\beta}(20.5)\,, \tag{3}$$

where V_M is the molar volume in cm^3 and

$$a(V_M) = (27 - V_M)/6.5\,.$$

This implies that

$$\Theta_D(V_M) = (20.5/V_M)^{1/3}\, a(V_M)\, \Theta_D(20.5)\,. \tag{4}$$

The values computed using this equation, although larger, agree within the combined errors with those taken from specific-heat measurements by Ahlers[41] (Fig. 15). The calorimetric values determined by Edwards and Pandorf[25] and the elastic values determined by Crepeau *et al.*[5] and Franck and Wanner[29,42] are also indicated.

A Θ_D of $19.5\ ^{+2}_{-3}$ K was calculated for bcc ^{3}He at 21.6 cm^3/mole using Eq. (2). The Debye velocity $I^{-1/3}$ was determined by numerically integrating the expression for I over $\frac{1}{16}$ of the reference sphere using $\frac{1}{2}^\circ$ intervals for both angle variables and using the three sound velocities at each of the grid points determined by the elastic moduli. The large uncertainty in Θ_D arises from the uncertainty in the modulus determining the velocity of the soft transverse mode in the ⟨101⟩ direction, namely, $\frac{1}{2}(C_{11} - C_{12})$.

Sample and Swenson[43] and Pandorf and Edwards[44] have found in measurements of the bcc-^{3}He specific heat an anomalous contribution at temperatures less than ~0.5 K. According to Debye theory, near absolute zero the specific heat should go as $(T/\Theta_D)^3$. Assuming that this T^3 dependence should hold at temperatures such that $T/\Theta_D \lesssim 0.02$ (as is the case for hcp ^{4}He[41]), the specific heat is split into two components: the "phonon" contribution proportional to T^3 and the excess (anomalous) contribution. If the specific heat is expressed in terms of a temperature-dependent Θ_D, the anomalous component contains all of the low-temperature

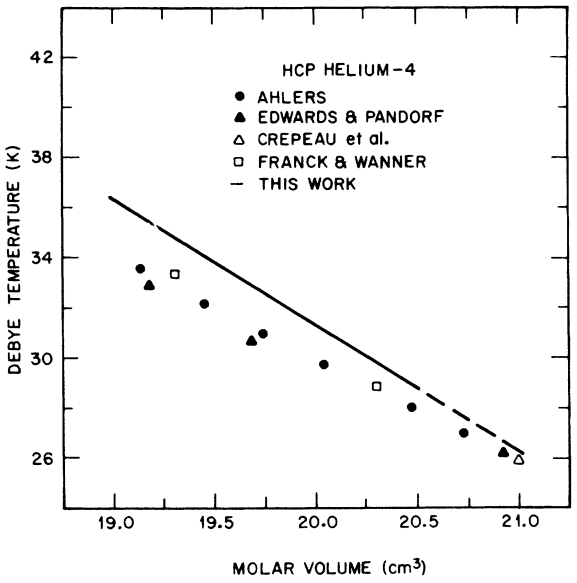

FIG. 15. Comparison of the Debye temperatures determined by Eqs. (1) and (4) with the values taken from specific-heat measurements by Ahlers (Ref. 41). Results from Refs. 25, 5, and 29 are also indicated.

dependence, while the "phonon" component is equal to the maximum value of $\Theta_D(T)$. At 21.46 cm^3/mole, Sample and Swenson find this maximum value to be ~25 K.

Hendricksen *et al.* [45] have investigated the temperature dependence of $\Theta_D(T)$ through the relation

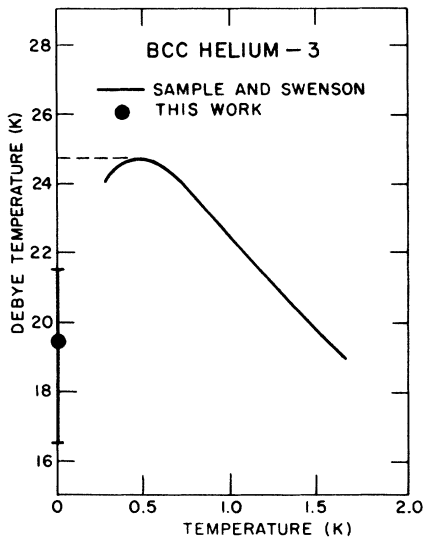

FIG. 16 Comparison of the bcc-^{3}He Θ_D at 21.6 cm^3/mole determined by the elastic constants and $\Theta_D(T)$ interpolated from the specific-heat measurements of Sample and Swenson (Ref. 43).

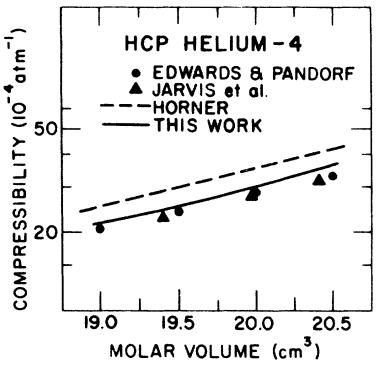

FIG. 17. Comparison of the volume compressibilities determined by Eqs. (5) and (6) with the experimental values given by Edwards and Pandorf (Ref. 25) and Jarvis *et al.* (Ref. 49) and the theoretical results of Horner (Ref. 48).

$$\left(\frac{\partial P}{\partial T}\right)_V = \frac{\gamma C_V}{V_M} = \frac{234\gamma R}{V_M}\left(\frac{T}{\Theta_D(T)}\right)^3$$

and have verified that the decrease in $\Theta_D(T)$ at low temperatures is a real effect associated with the lattice specific heat of pure ^{3}He.

The zero-temperature Debye Θ determined by the present work is in qualitative agreement with these experiments, Fig. 16, and indicates that the anomaly is in the phonon spectrum itself. This is consistent with the findings of Thomlinson[46] in his work on the thermal conductivity of bcc ^{3}He.

Horner's[37] calculation of the bcc-^{3}He phonon spectrum which includes the leading anharmonic corrections to the self-consistent harmonic approximation shows an anomalous dispersion for long wavelengths which causes a fall off of $\Theta_D(T)$ at low temperatures.

Compressibility

The volume compressibility in the hexagonal system in terms of the elastic moduli is given by[47]

$$\beta_V = (C_{11} + C_{33} - C_{66} - 2C_{13})/[C_{33}(C_{11} - C_{66}) - C_{13}^2] .$$

But because of relation (1), C_{13} can be eliminated reducing this expression to

$$\beta_V = 3/[4(C_{11} - C_{66}) - C_{33}] . \qquad (5)$$

Due to the large uncertainty in C_{33}, the uncertainty in β_V at 20.5 cm^3/mole determined by this expression is estimated to be 5%. The volume dependence of the ^{4}He compressibility, using (3), can be written

$$\beta_V(V_M) = (V_M/20.5)\, a^{-2}(V_M)\, \beta_V(20.5) . \qquad (6)$$

A comparison with the theory of Horner[48] and with the compressibilities deduced by Edwards and

Pandorf[25] from their measurements of the specific heat and PVT data along the melting curve given by Grilly and Mills[24] is made in Fig. 17. Also shown are the values determined by Jarvis *et al.*[49] from their measurements of $(\partial P/\partial T)_V$.

In the cubic system, the expression for the volume compressibility is

$$\beta_V = 3/(C_{11} + 2C_{12}) .$$

Substitution of the ^{3}He values for C_{11} and C_{12} at 21.6 cm^3/mole yields a compressibility of 27.8 $\times 10^{-4}$ atm^{-1}. This agrees to within the 2% error with the value determined by Straty and Adams[50] from measurements of $P(T)$ for various molar volumes and also agrees well with the theoretical calculations of Horner[48] and Hetherington, Mullin, and Nosanow.[51]

V. SUMMARY

Longitudinal and transverse sound velocities have been measured in low-density x-ray-oriented single crystals of hcp ^{4}He and bcc ^{3}He. The crystals were grown at nearly constant pressure by slowly lowering the temperature of one end of a plastic freezing cell. X-ray photographs of the samples showed that generally the crystals were of the highest quality and provided sufficient information to unambiguously determine the crystal orientation. The measured sound velocities were compared with the theory and showed at least qualitative agreement, provided in the case of bcc ^{3}He that the theory included the anharmonic corrections to the Hamiltonian. The elastic moduli for hcp ^{4}He at 20.5 cm^3/mole and bcc ^{3}He at 21.6 cm^3/mole were determined. The moduli for the cubic structure imply very soft transverse modes near the $\langle 101 \rangle$ direction and a Θ_D in agreement with previous experiments. These soft modes lead to an anomalous phonon spectrum which accounts for the low-temperature specific-heat anomaly. The calculated Θ_D for ^{4}He and the volume compressibilities for ^{3}He and ^{4}He are in agreement with other measurements.

ACKNOWLEDGMENTS

The author wishes to express his gratitude to his sponsor, Dr. J. A. Munarin, for his support and advice; to Dr. F. M. Lurie, Dr. J. C. Swihart, S. C. Ems, and H. V. Lauer for their interest and many helpful suggestions; and also to D. A. Greywall for her assistance in the taking of data.

---

†Work supported by the National Science Foundation.

*Present address: Bell Telephone Laboratories, Murray Hill, N.J. 07974.

[1]J. Wilks, *The Properties of Liquid and Solid Helium* (Clarendon, Oxford, England, 1967).

[2]A. I. Shal'nikov, Zh. Eksperim. i Teor. Fiz. 41, 1056 (1961) [Sov. Phys. JETP 14, 753 (1962)].

[3]L. P. Mezhov-Deglin, Zh. Eksperim. i Teor. Fiz. 49, 66 (1965) [Sov. Phys. JETP 22, 47 (1966)].

[4]O. W. Heybey and D. M. Lee, Phys. Rev. Letters 19, 106 (1967).

[5]R. H. Crepeau, O. Heybey, D. M. Lee, and Stanley A. Strauss, Phys. Rev. (to be published).

[6]J. S. Dugdale, in *Physics of High Pressures and the Condensed Phase*, edited by A. van Itterbeck (North-Holland, Amsterdam, 1965), Chap. 9.

[7]S. C. Fain and D. Lazarus, Phys. Rev. A 1, 1460 (1970).

[8]V. J. Minkiewicz, T. A. Kitchens, F. P. Lipschultz, R. Nathans, and G. Shirane, Phys. Rev. 174, 267 (1968).

[9]T. O. Brun, S. K. Sinha, C. A. Swenson, and C. R. Tilford, in Proceedings of the IAEA Conference on Inelastic Neutron Scattering, Copenhagen, 1968 (unpublished).

[10]R. Wanner and J. P. Franck, Phys. Rev. Letters 24, 365 (1970).

[11]R. A. Guyer and E. M. Hogan, Solid State Commun. 5, 909 (1967).

[12]E. M. Hogan, R. A. Guyer, and H. A. Fairbank, Phys. Rev. 185, 356 (1969).

[13]J. H. Vignos and H. A. Fairbank, Phys. Rev. Letters 6, 265 (1961).

[14]J. H. Vignos and H. A. Fairbank, Phys. Rev. 147, 185 (1966).

[15]F. P. Lipschultz and D. M. Lee, Phys. Rev. Letters 14, 1017 (1965).

[16]F. P. Lipschultz and D. M. Lee, in *Proceedings of the Tenth International Conference on Low Temperature Physics* (VINITI, Moscow, 1967), Vol. 1, p. 309.

[17]D. S. Greywall and J. A. Munarin, Phys. Letters 31A, 469 (1970).

[18]D. S. Greywall and J. A. Munarin, Phys. Rev. Letters 24, 1282 (1970); 25, 261(E) (1970); because of a typographical error in the erratum, Θ_D was given as 19.95^{+2}_{-3} K in place of 19.5^{+2}_{-3} K.

[19]V. K. Tkachenko and A. I. F. Filimonov, Cryogenics 2, 359 (1962).

[20]E. J. Walker, Rev. Sci. Instr. 30, 834 (1959).

[21]Emerson and Cummings, Inc., Canton, Mass.

[22]The Polymer Corporation, Reading, Pa.

[23]J. E. Vos and R. Kingma, Cryogenics 7, 50 (1967).

[24]E. R. Grilly and R. L. Mills, Ann. Phys. (N.Y.) 8, 1 (1959).

[25]D. O. Edwards and R. C. Pandorf, Phys. Rev. 140, A816 (1965).

[26]C. C. Ackerman and R. A. Guyer, Ann. Phys. (N. Y.) 50, 128 (1968).

[27]B. D. Cullity, *Elements of X-Ray Diffraction* (Addison-Wesley, Reading, Mass., 1959).

[28]S. C. Fain and D. Lazarus, J. Appl. Phys. 41, 1451 (1970).

[29]J. P. Franck and R. Wanner, Phys. Rev. Letters 25, 345 (1970).

[30]J. E. Vos, thesis (Technische Hogeschool Delft, Netherlands, 1968) (unpublished).

[31]N. S. Gillis, T. R. Koehler, and N. R. Werthamer, Phys. Rev. 175, 1110 (1968).

[32]L. H. Nosanow and N. R. Werthamer, Phys. Rev.

Letters 15, 618 (1965).
[33]It is to be noted that these values differ slightly from the preliminary values given in Ref. 18.
[34]L. R. Testardi, T. B. Bateman, W. A. Reed, and V. G. Chirba, Phys. Rev. Letters 15, 250 (1965).
[35]F. W. DeWette, L. H. Nosanow, and N. R. Werthamer, Phys. Rev. 162, 824 (1967).
[36]T. R. Koehler, Phys. Rev. Letters 18, 654 (1967); and private communication.
[37]H. Horner, Phys. Rev. Letters 25, 147 (1970).
[38]H. Horner (private communication).
[39]T. R. Koehler and N. R. Werthamer (private communication).
[40]F. I. Fedorov, *Theory of Elastic Waves in Crystals* (Plenum, New York, 1968).
[41]G. Ahlers, Phys. Rev. A 3, 696 (1971).
[42]D. S. Greywall (unpublished).
[43]H. H. Sample and C. A. Swenson, Phys. Rev. 158, 188 (1967).
[44]R. C. Pandorf and D. O. Edwards, Phys. Rev. 169, 222 (1968).
[45]P. N. Henrickson, M. F. Panczyk, S. B. Trickey, and E. D. Adams, Phys. Rev. Letters 23, 518 (1969).
[46]W. C. Thomlinson, Phys. Rev. Letters 23, 1330 (1969).
[47]J. F. Nye, *Physical Properties of Crystals* (Clarendon, Oxford, England, 1957).
[48]H. Horner, Phys. Rev. A 1, 1722 (1970).
[49]J. F. Jarvis, D. Ramm, and H. Meyer, Phys. Rev. 170, 320 (1968).
[50]G. C. Straty and E. D. Adams, Phys. Rev. 169, 232 (1968).
[51]J. H. Hetherington, W. J. Mullin, and L. H. Nosanow, Phys. Rev. 154, 175 (1967).

PHYSICAL REVIEW A VOLUME 3, NUMBER 6 JUNE 1971

Microscopic Method for Calculating Memory Functions in Transport Theory*

Gene F. Mazenko
Department of Physics and Research Laboratory of Electronics, Massachusetts Institute of Technology, Cambridge, Massachusetts 02139
(Received 16 October 1970)

It is shown how the method of thermodynamic Green's functions can be used to approximate the memory function associated with the equilibrium-fluctuation function $S_c(\vec{r}-\vec{r}', \vec{p}\vec{p}', t-t') \equiv \langle [f(\vec{r}\vec{p}t) - \langle f(\vec{r}\ \vec{p}t)\rangle][f(\vec{r}'\vec{p}'t') - \langle f(\vec{r}'\vec{p}'t')\rangle]\rangle$, where $f(\vec{r}\vec{p}t)$ is the phase-space distribution operator. We obtain an approximation for the memory function for a gas, in the low-density limit, that is valid for all distances and times, satisfied various relevant symmetry conditions and sum rules, reduces for long times and distances to the Boltzmann collision operator, and gives results completely consistent with the conservation laws governing the system. We also indicate how these methods can be extended to treat other types of systems.

I. INTRODUCTION

The usefulness of time-dependent correlation functions in describing deviations from equilibrium in many-particle systems is well known. In particular, the equilibrium-fluctuation function for the classical phase-space distribution operator

$$S_c(\vec{r}-\vec{r}', \vec{p}\vec{p}', t-t') \equiv \langle [f(\vec{r}\vec{p}t) - \langle f(\vec{r}\vec{p}t)\rangle][f(\vec{r}'\vec{p}'t) - \langle f(\vec{r}'\vec{p}'t)\rangle]\rangle , \tag{1.1}$$

where

$$f(\vec{r}\vec{p}t) \equiv \sum_{i=1}^{N} \delta(\vec{r}-\vec{r}_i(t))\delta(\vec{p}-\vec{p}_i(t)) , \tag{1.2}$$

describes all information obtained from light- and neutron-scattering experiments,[1,2] gives the linear response of a system to a weak external probe,[2,3] and its space-time Fourier transform contains all information related to linearized hydrodynamics.[4-7] For these reasons, there is considerable interest in developing methods for determining S_c. In order to avoid unphysical secular effects, these methods are usually based on making approximations for the inverse of S_c. This inverse is related to the memory function $\varphi(\vec{r}-\vec{r}', \vec{p}\vec{p}', t-t')$ by the generalized Langevin equation derived formally by Mori[8,9]:

$$\left(\frac{\partial}{\partial t} + \frac{\vec{p}\cdot\nabla_r}{m}\right) S_c(\vec{r}, \vec{p}\vec{p}', t) - \int_0^t d\bar{t} \int d^3\bar{r}\, d^3\bar{p}\, \varphi(\vec{p}\varphi(\vec{r}-\bar{\vec{r}}, \vec{p}\bar{\vec{p}}, t-\bar{t}) S_c(\bar{\vec{r}}, \bar{\vec{p}}, \vec{p}', \bar{t}) = 0 . \tag{1.3}$$

We will be particularly interested in the Fourier-Laplace transform of this equation:

$$\left(z - \frac{\vec{k}\cdot\vec{p}}{m}\right) S_c(\vec{k}, \vec{p}\vec{p}', z) - \int d^3\bar{p}\, \varphi(\vec{k}, \vec{p}\bar{\vec{p}}, z) \times S_c(\vec{k}, \bar{\vec{p}}\vec{p}', z) = -\tilde{S}_c(\vec{k}, \vec{p}\vec{p}') , \tag{1.4}$$

where the complex fluctuation function is defined by

$$S_c(\vec{k}, \vec{p}\vec{p}', z) = i \int d^3r\, e^{-i\vec{k}\cdot\vec{r}} \int_0^{+\infty} dt\, e^{+izt} S_c(\vec{r}, \vec{p}\vec{p}', t) , \tag{1.5}$$

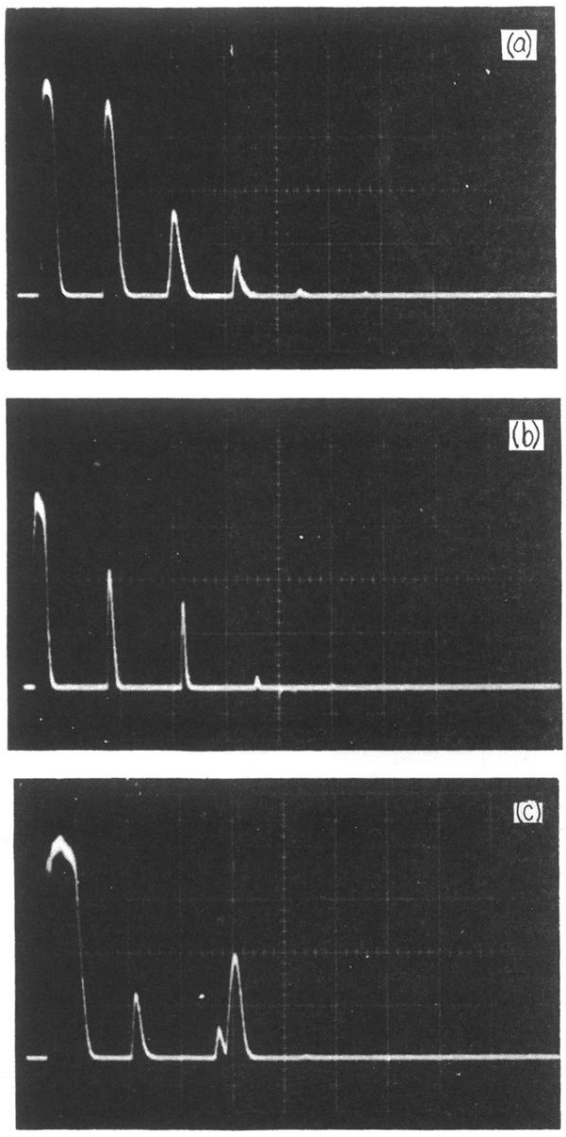

FIG. 12. Oscilloscope traces showing transmitted (first) and received pulses. (a) Longitudinal signal in bcc ^{3}He (50 μsec/division). (b) Transverse signal in hcp ^{4}He (100 μ sec/division). (c) Signal in hcp ^{4}He showing both longitudinal and transverse (last pulse) echoes (50 μsec/division).

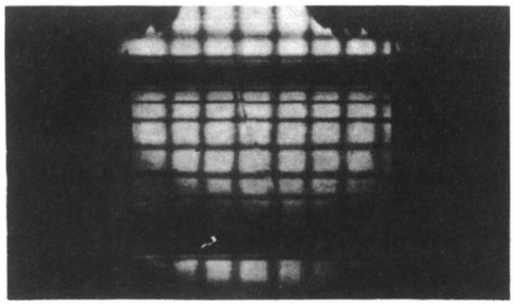

FIG. 6. Photograph taken during the growth (at constant pressure) of a solid helium sample. The solid is to the left of the nearly vertical solid-liquid interface in the middle of the photograph.

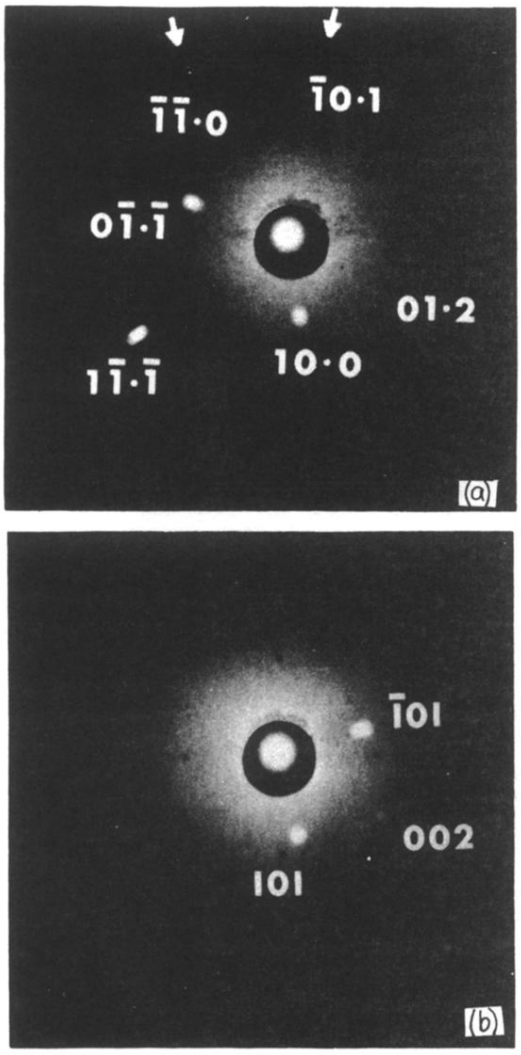

FIG. 7. Transmission Laue photographs of (a) a single hcp-helium-4 crystal (20.5 cm^3/mole) and (b) a single bcc-helium-3 crystal (21.6 cm^3/mole). The crystal-to-film distance was 5 cm.